INVESTIGATION OF THE MECHANISM OF STRESS CORROSION OF ALUMINUM ALLOYS

Bureau of Naval Weapons Contract Now64-0170c

Third Quarter Report

(Period of June 1, 1964 to November 30, 1964)

48 P

Reported by: G. C. English
G. C. English

J. McHardy

Approved by: E. H. Hollingsworth
E. H. Hollingsworth

Table of Contents

SYNOPSIS

During the third quarter, cathodic protection studies were emphasized. The many experimental conditions affecting these studies were explored, and, it is believed, largely resolved. Experimental techniques that provide reproducible and reliable measurements were developed.

Extensive measurements were made upon 2-inch thick 7075 alloy plate in two tempers, one (-T6) susceptible to stress corrosion, and one (-T73) not susceptible. For these measurements, specimens taken in the short-transverse direction, to provide maximum susceptibility, were tested in an aggressive electrolyte consisting of an aqueous solution of chlorides acidified to pH 1. In this electrolyte, a susceptible specimen stressed to 75% of its yield strength failed by stress corrosion in approximately one hour, and a stressed, non-susceptible specimen failed by general corrosion in 48 hours or less. An aggressive electrolyte was required primarily to permit measurements within a reasonable period.

Two pertinent potentials of cathodic protection were found, the first one 150 millivolts negative to the corrosion potential, and the second, and much more sharply defined one, 575 millivolts negative to this potential. Pitting ceased when a specimen was polarized cathodically beyond the first potential, but polarization to the second potential was required to eliminate stress corrosion. A 7075-T6 alloy specimen stressed to 75% of its yield strength and polarized to the second potential for as long as 400 hours was completely protected from stress corrosion and

showed no detectable corrosion of any type. Polarization to a potential more negative than the second potential of cathodic protection led to overprotection and associated alkaline attack.

Future work is being directed, first, toward providing additional evidence that the results reflect microstructural features (rather than environmental conditions), and second, toward identifying these features. Attention will be given to further metallographic examinations with both the light and electron microscope. An interesting possibility is that the first potential of cathodic protection corresponds to the "critical" potential described by Kolotyrkin for pitting corrosion of a metal in a solution containing halide ions; and that the second potential corresponds to a "critical" potential for a second, more anodic phase.

INTRODUCTION:

This report summarizes work during the period, June 1 to November 30, 1964*. In this period, 3,018 man hours were spent on the contract. This work was spent mainly on the development of a suitable experimental technique for the precise measurement of the potentials required for cathodic protection, as a means of establishing the potential of phases in an alloy; and to measurement of these potentials in 7075 alloy in tempers susceptible and non-susceptible to stress corrosion.

MATERIALS:

Tests were restricted to 7075 alloy. With one exception, which is noted later, specimens were taken in the short-transverse direction from a production lot of 2-inch thick plate of 7075-T651 alloy. Blanks from this plate (1/4" x 1/4" x 2") were reheat-treated and artificially aged to the -T6 and -T73 tempers, and then machined into 1/8-inch diameter tensile specimens. The chemical analysis of the plate and the tensile properties and electrical conductivities of the -T6 and -T73 tempers are summarized in Table I.

The use of a new lot of plate was required to provide specimens sufficiently susceptible to stress corrosion. Even in the aggressive solution used for the cathodic protection studies, specimens taken from the 1/4-inch thick plate ordered for the contract did not fail until after considerable general corrosion had taken place.

---

* The contract was extended from 12 to 14 months and the due date for the third quarterly report was changed to December 6, 1964.

GENERAL PROCEDURE FOR CATHODIC PROTECTION STUDIES:

In the cathodic protection studies, stressed or unstressed specimens were cathodically polarized to selected potentials by means of a potentiostat. The progress of corrosion was followed by electrical resistance measurements made periodically throughout a test. Unstressed specimens were kept in test for a period sufficient to establish the slope of the resistance-time curve; this slope provided a measure of corrosion rate. The period required varied from hours or days up to a week or more, depending upon the potential. Specimens stressed to 75% of the yield strength and polarized to a potential less negative than that required for protection generally failed by stress corrosion within a day or two. Those held at potentials in the protective range showed very little change in resistance or appearance other than a gradual loss in reflectivity and the development of a dark colored surface; these specimens were kept in test up to 400 hours. At the conclusion of a test, one of two procedures was adopted to provide additional information about the amount of corrosion, the stress level and the susceptibility of the specimen to stress corrosion. In some instances, a specimen was unloaded to check the stress level and then the loss in tensile strength was determined, while, in other cases, the potential was shifted to a more positive value and the time required for stress corrosion failure was determined. Most specimens were examined metallographically to determine the nature and type of corrosion.

SOLUTION:

The test solution contained 1.00 mole per liter of sodium chloride and 0.21 mole per liter of $AlCl_3$ added as $AlCl_3 \cdot 6H_2O$

(5% $AlCl_3 \cdot 6H_2O$). The pH was adjusted to 1.0 by the addition of concentrated hydrochloric acid. A pH of 1.0 was selected because it provided a measurable rate of general corrosion, and, equally important, because it produced stress-corrosion cracking rapidly in specimens of 7075-T6 stressed in the short-transverse direction. Because aluminum chloride was introduced into the solution as a corrosion product in varying degrees in most of the tests, it appeared reasonable to start with a solution in which aluminum chloride initially was present at a level high enough so that the concentration would remain essentially constant throughout a test.

APPARATUS:

The apparatus and circuits used for the cathodic protection experiments are shown in Figures 1 and 2.

The tests were conducted in battery jars, each containing 9 liters of solution. A sheet of Plexiglas with suitable openings was used to cover each jar and support the specimen, the anodes and a thermometer. The anodes were located in individual compartments separated from the main portion of the solution by fritted glass discs of medium porosity. Aluminum of 99.99% purity was used for the anodes in preference to platinum because aluminum chloride was considered less objectionable than chlorine as an anode reaction product. The solution in the anode compartments was discarded each day and replaced with fresh solution. The main portion of the battery jar was, in effect, the cathode compartment of the cell.

One of the objects in using a large volume of solution was to minimize the pH increase produced by the cathodic reactions. Daily pH adjustment by adding a few milliliters of concentrated hydrochloric acid was sufficient to hold the pH constant to within $\pm$ 0.05 pH unit or better. An entirely fresh solution was made up from time to time especially after an appreciable amount of corrosion had occurred.

The potentiostats used in the present work were electronic instruments with chopper-stabilized operational amplifiers, similar in design to the instrument described by Booman (1). A recorder was used to provide a continuous record of the current, and by means of a timer and relay, the recorder was also used tc monitor the continuity of a specimen several times each hour. A 1 ohm or 0.1 ohm shunt connected across the two potential terminals of the specimen was used for this purpose. A negligible current flowed through the shunt until a specimen broke. When a specimen broke, a measurable portion of the protection current flowed through the shunt and provided an indication on the recorder.

The specimens were stressed in standard fixtures for 1/8-inch tensile specimens. The electrical resistance measurements required that a specimen be insulated from the stressing frame and that current and potential leads be attached. As mentioned in the first quarterly report, either an anodic hard coating or ceramic washers provided electrical insulation between the specimen and the frame. The necessary leads were attached by percussion welding.

A photograph of a specimen is shown in Figure 3. The two potential leads needed for resistance measurements were attachod,

one at each end of the specimen, in the area between the threads and the reduced section. A separate lead similarly located was used as a direct connection to the potentiostat. With this arrangement IR drops in the leads carrying the resistance test current do not interfere with the operation of the potentiostat, and vice versa. The current leads for the resistance measurement were welded to the cap nuts which are used to mount the specimen in the stressing fixture. Corrosion tests and measurements to evaluate the loss in strain demonstrated that the modified specimen and frame used in the present tests is equivalent in performance to the standard specimen and frame.

Figure 3 also shows a specimen ready for immersion in the test solution. Wax stop-off has been applied so that the entire reduced section of the specimen is exposed to the solution. Hydrogen bubbles occasionally tended to cling to the metal-wax junction. There was a remote possibility that such clinging bubbles might act as a temporary screen and thus allow a stress crack to initiate. Accordingly, the junction between the wax and the exposed area was established outside the uniform part of the reduced section in order to minimize the possibility of spurious attack occurring in the region of highest stress.

Luggin capillaries were mounted through holes drilled in the side members of the frame and each tip was positioned 3 millimeters from the surface of the specimen. The tip diameter was about 1 millimeter. Smaller capillaries positioned 1 millimeter from the specimen were used initially but were finally discontinued when it was found that they tended to catch stray

hydrogen bubbles evolved from the surface of the specimen. The resulting open circuit condition prevented the potentiostat from functioning properly with the result that the experiment in progress was lost. The utmost in reliability is imperative where long-time runs are conducted. The use of two capillaries was simply a precaution rather than a necessity. Both capillaries were connected to the same reservoir, in which a saturated calomel electrode was located.

All the potential measurements included in this report are in terms of the saturated calomel reference electrode. The European sign convention is used in which the potential of an active metal is given a negative sign. A Leeds and Northrup 8687 potentiometer was used to measure electrode potentials.

CORRECTION FOR IR DROPS:

At the current densities encountered, it was necessary to apply a correction for the IR drop in the solution between the capillary tip and the specimen. By means of a movable capillary, it was found that the potential distribution followed the ideal law for concentric cylinders for distances up to about 1 centimeter from the surface of the specimen. The resistance could be calculated from the following equation:

$$R = \frac{\rho}{2\pi} \ln (r_2/r_1) \qquad (1)$$

where ρ is the resistivity of the solution (7.86 ohm-cm at 25°C), r_1 is the radius of the specimen in centimeters, r_2 is the corresponding radius out to the tip of the Luggin capillary and

R is the resistance of an annular cylinder of solution surrounding the specimen and having the following dimensions: height of 1 centimeter, inner diameter of $2r_1$ and outer diameter of $2r_2$. The correction to the measured potential is then the product I x R, where R is given by equation (1) and I is the current flowing to the corresponding area. Expressed in terms of the current density i the correction is:

$$IR = i\,2\pi r_1 \frac{\rho}{2\pi} \ln \frac{r_2}{r_1} = i r_1 \rho \ln \frac{r_2}{r_1} \qquad (2)$$

For a 3 millimeter spacing, equation (2) becomes:

$$IR = 1.32\ i \qquad (3)$$

Considering the IR drop to be positive in sign and the measured potential E_m to be negative in sign, the corrected potential of the cathode E_c is:

$$E_c = E_m + (IR) \qquad (4)$$

E_m is equal in magnitude to the control potential setting on the potentiostat; therefore, it is evident that the control potential setting must vary with the current density if E_c is to be constant. This adjustment was made manually as required. Typical overnight variations in current were so small that deviations from the desired control potential were generally less than $\pm$ 0.005 volts.

The correction could have been performed automatically; one of the simplest ways to obtain a signal proportional to the current would be to use a transmitting slide wire on the current recorder, but this refinement did not seem worthwhile.

RESISTANCE MEASUREMENTS:

The resistance measurements were made by the potentiometer method (Figure 2). In this method, a specimen is connected in series with a standard resistance R_s and a constant test current is passed through both resistances. The potential E_x across the unknown is compared with the potential E_s across the standard resistance and the resistance of the specimen R_x is calculated from the expression:

$$R_x = \frac{E_x}{E_s} R_s$$

E_x and E_s were measured with a Leeds and Northrup type K3 potentiometer No. 7553-5 and a No. 2430-a galvanometer. R_s was a Rubicon 0.001 ohm standard resistance having a 10 ampere current rating.

A test current of 1.2 amperes was used since this seemed to be a satisfactory compromise between heating effects, which increase with the square of the current, and signal size which is proportional to current. The requirement of a constant test current was obtained by using a 6-volt storage battery with a 5-ohm resistance in series to limit the current flow.

Thermal emfs and the small emf due to the cathodic protection current flow through the specimen were compensated for by using the galvanometer defection obtained with the test current off and with the potentiometer set at zero as the null point for the actual measurement.

The temperature of the room was controlled to about ± 1°C and the solution temperature was measured on a thermometer graduated in intervals of 0.02°C. The resistance readings were then corrected to 20°C using the expression:

$$R_{20} = \frac{R_T}{1 + \alpha(T - 20)}$$

where T is the temperature of the solution in degrees centigrade, R_T is the resistance of the specimen at a temperature of T°C, R_{20} is the calculated resistance at 20°C and α is the temperature coefficient of resistance. This coefficient can be determined experimentally or it can be calculated from a measurement of the conductivity using the expression:

$$\alpha = \frac{(\text{conductivity in \% IACS})}{61.00} \quad 0.00403$$

Both methods gave similar results. Values of 0.00205 and 0.00254 for the -T6 and -T73 tempers respectively were obtained on the specimens used in the present tests.

The results for a typical run are shown in Figure 4. The overall precision of the resistance measurement appeared to be of the order of 0.1% judging from the deviation of values from the best line through the data points. This precision corresponds to an overall error of 0.2 microvolt in measuring E_x.

For very low corrosion rates, the accuracy of the rate measurement becomes directly proportional to the test period. Since something around 400 hours was about the maximum period employed, the uncertainty in a rate measurement would be about

$\pm$0.0005 microhms per hour. The relation between the resistance change and the rate of penetration given in Appendix I indicates that uniform corrosion producing 0.0005 microhms change per hour is equivalent to a corrosion rate of 0.001 inches per year.

RESULTS:

The basic results of the investigation are summarized in Figures 5 and 6. Figure 5 shows the effect of potential on the time to failure of 1/8-inch diameter tensile specimens of 7075-T6 stressed to 75% of the yield strength. Data for the -T73 temper does not appear in Figure 5 because none of the specimens in this temper were susceptible to stress corrosion. Figure 6 shows the effect of potential on the corrosion rate of 7075-T6 and -T73 for both stressed and unstressed specimens.

Figure 5 shows that stressed specimens of 7075-T6 polarized to potentials less negative than -1.32 v failed by stress corrosion within 15 hours. Specimens polarized between 1.32 and 1.45 v did not fail. Those polarized at or more negative than -1.45 v failed by overprotection. The specimen held at -1.325 v showed no detectable sign of stress corrosion even after 400 hours. This specimen was tensile tested and showed only a 2% loss in tensile strength, which probably is negligible.

Specimens first held in the range -1.32 to -1.45 v showed normal failure times when the potential was shifted to less negative values. For example, after the test at -1.375 v had been continued for 304 hours with no appreciable corrosion, the potential was changed to -1.15 v; failure then occurred in 4.3

hours. In a second test, a specimen protected at -1.320 volts failed in 12 hours when the potential was changed to -1.29 volts. For both specimens, time to failure at the less negative potential is indicated in Figure 5 by the half-filled circles; it is evident that both of the points fall close to the curve for normal specimens held at a single constant potential.

Alkaline attack or overprotection which occurred at potentials of -1.45 v or more negative produced characteristic smooth-bottomed pits and general thinning which ultimately caused the specimen to fail.

Figure 6 provides further evidence of a pertinent potential of cathodic protection in the neighborhood of -1.325 v. In fact, it defines the upper limit of this potential more precisely. The corrosion rate at -1.375 v was considered measurable, that is, greater than the possible experimental error, while the rate at -1.325 was considered less than the possible experimental error. Thus the upper limit evidently lies between -1.325 and -1.375. The data in Figure 5 indicate a lower limit between -1.290 and -1.320 v.

Figure 6 also provides evidence of a second pertinent potential of cathodic protection. This potential lies in the neighborhood of -0.90 v which is about 0.15 v negative to the corrosion potential. Polarization to this potential reduced the corrosion rate by a factor of almost 1000. (The curve in Figure 5 has been drawn to indicate a break at a potential in the neighborhood of -0.90 v; but in the absence of Figure 6, there is no valid reason for doing so.)

In the range, -0.9 to -1.2 v, the curve in Figure 6 has been dashed. In this range, the corrosion rate was very small, and, in this situation, the accuracy of a rate measurement is proportional to the length of the test. The points at -1.325 and -1.375 v were run for 17 and 13 days, respectively. They are more reliable than the points between -1.0 and -1.2 v which were run no longer than 5 days. In the region of overprotection, the corrosion rate increased rapidly as the potential became more negative. The corrosion rate at -1.55 v was estimated from the reduction in diameter.

The corrosion rates plotted in Figure 6 were obtained as the slopes of the corresponding resistance-time curves. For the scale used in Figure 6, the relation between corrosion rate in microhms per hour and potential is sufficiently similar for both -T6 and -T73 tempers so that it was not necessary to draw separate curves. It is to be emphasized, of course, that similar resistance-time curves do not imply the same corrosive attack. This point is demonstrated by the micrographs in Figure 7 comparing the different types of attack of freely corroding -T73 and -T6 temper specimens. In the present case, the effects of weight loss and uniformity on resistance evidently tended to compensate.

No distinction between stressed and unstressed specimens was made in Figure 6. In fact no difference was expected for specimens in the -T73 temper because these specimens were not susceptible to stress corrosion. For the -T6 temper, the effect of stress was generally only apparent in the latter 25 or 50% of the life of

a specimen. In this period the rate of resistance change of a stressed -T6 specimen increased markedly while that of an unstressed specimen remained unchanged. If data taken during this phase had been used, the curves for stressed and unstressed -T6 temper specimens would not have been similar.

The accelerating effect of stress for freely corroding specimens is shown in Figure 8. During the first stage of corrosion, the curves apparently reflect the initial surface condition of the specimens, before equilibrium corrosion conditions were reached. This induction period was ignored in establishing corrosion rates. In cathodically protected stressed specimens, the overall change in resistance was generally less than illustrated in Figure 8, but the rate of change was more nearly exponential. Also, the curves for unstressed and stressed specimens coincided for a longer period initially, as mentioned earlier.

Runs where corrosion took place led to contamination of the test solution with the alloying elements of 7075. It was recognized that copper ions in solution might affect the corrosion behavior. The data in Table II show that corrosion products caused some acceleration in stress corrosion but had relatively little effect on the corrosion rate of unstressed specimens.

The depolarizing effect caused by cupric ions or by the corrosion product of 7075 is evident in the current-time curves in Figure 9. Blanks from the original 0.250-inch thick plate were used for these measurements. This depolarizing effect made it easy to detect contamination, and solutions from a run in which

corrosion occurred were not re-used. Presumably, copper deposited on the surface of a specimen and provided a cathode at which hydrogen reduction proceeded more rapidly. It is interesting to note in Figure 9 that copper ion added alone was more effective than an addition of the same amount of copper obtained by dissolving 7075. Although the addition of corrosion product made the current requirement to maintain -1.15 v several fold greater than the current requirements to reach a protective potential in uncontaminated solution, the time to failure at -1.15 remained relatively short indicating that potential rather than current density is the significant factor in cathodic protection.

DISCUSSION:

Without much question, the most significant result of the present investigation is that stress corrosion of a highly susceptible aluminum alloy in a highly aggressive environment can be prevented by cathodic protection, evidently, for an indefinitely long period. The important question naturally is whether this result reflects microstructural features, or environmental changes, or both. Future experimental work is required to answer this question conclusively. At the same time, the results already obtained, although not conclusive, do provide evidence bearing on the question.

The fact that the protective potential in the neighborhood of -1.325 v is rather sharply defined provides evidence that this potential is related to microstructural features. Such a potential would be expected from the simple concept of a single

anodic phase segregated along a continuous path as a principal factor in stress corrosion. It would also be expected from the more involved theory of critical potentials advanced by Kolotyrkin (2) and others (3).

A brief discussion of this theory with respect to the protective potential in the neighborhood of -0.9 v as well as to that in the neighborhood of -1.325 v is profitable. Substantially more evidence in support of this theory can be advanced for the lower protective potential; indirectly, this evidence then supports the application of the theory to the more negative potential.

In its simplest terms, the theory states that pitting attack of a pure metal by a specific anion such as a halide ceases abruptly when the potential becomes more negative than a critical value. When this value is reached, the anion no longer enters into the anodic reaction. In effect, the polarization curve consists of two branches, one parallel to the potential axis, and one parallel to the current axis. Consequently, the current increases rapidly as the potential becomes more positive than the critical value and decreases rapidly as the potential becomes more negative than this value.

The similarity of these anodic polarization curves to the curves in Figure 6 is evident. Polarization to potentials in the neighborhood of -0.9 v decreased the corrosion rate tremendously. Evidence that this decrease was accompanied by at least a substantial decrease in pitting attack is provided by the micrographs in Figure 10. Significantly, other investigators have also reported that

potentials of this magnitude generally provide cathodic protection to aluminum alloys in chloride or in acid solutions (4,5).

Actually the curves in Figure 6 may be viewed as a combination of two sets of anodic polarization curves of the type just discussed; and they have in fact been drawn with this consideration in mind.

Preliminary work on alloys prepared to represent the precipitating M-phase in 7075 alloy provides further evidence for the effect of microstructural features. In one of these alloys, corrosion appeared to be stopped by cathodic polarization to -1.32 v.

Conversely, arguments for an environmental effect can be advanced. These include such common considerations as the generation of the hydroxyl ions in cathodic reactions, the improvement in the stress-corrosion performance of aluminum alloys by alkalinity, and the greater stability of the oxide film in solutions less acid than the one used here (6). The most disturbing argument perhaps is that overprotection began at a potential (and current density) only slightly removed from that required for cathodic protection against stress corrosion. It can be argued of course that attributing the potential of cathodic protection to environmental factors alone requires a very careful balancing of many factors including the generation of hydroxyl ions and their diffusion; and that balancing of these factors would be improbable. In this connection the work of Peterson Smith and Brown (6) should be mentioned. These workers were not able to protect 7079-T6 alloy completely in neutral salt solution before overprotection was reached.

FUTURE WORK:

In the final quarter the investigation of 7075 will continue to be emphasized.

Further work will be pursued first of all to confirm that the protective potential represents microstructural conditions rather than a pH change. In addition to a direct approach in which the effect of bulk pH on the protective potential and on the stress-corrosion performance will be studied, supplementary experiments in which stirring is used to affect diffusion rates and experiments in which different anions or buffers are present may be employed.

Assuming that it will be possible to show that a pH change at the surface is not the principal factor in determining the protective potential, then a major part of the work will be directed to metallurgical aspects. This will include cathodic protection studies of compositions in the M-phase region of the Al-Zn-Mg-Cu system to test the hypothesis that stress corrosion is associated with corrosion of the M-phase.

More extensive metallographic studies will be made on both 7075-T6 and -T73 to observe the features of the microstructure that are attacked in specimens held at various potentials. If suitable experimental techniques can be worked out, the electron microscope will also be used.

In T. P. Hoar's theory of stress-corrosion cracking (8) one phase of the process is the anodic dissolution of locally yielding metal. This could correspond to the portion of the resistance-time curve where the stressed specimen undergoes accelerated corrosion

Experiments in which application of cathodic protection after accelerated attack has begun will be attempted. If this model is correct, the protection potential should be equivalent to that of unfilmed aluminum and therefore unattainable. However, it is recognized that failure to achieve protection could also be explained on the basis of the failure of the protection current to reach the root of the crack.

The effect of stress level on cathodic protection requirements has been neglected to date. If time permits, the effect on the protection potential of stress levels other than the 75%Y.S. level used in all the tests to date will be investigated.

APPENDIX I

Where corrosion is uniform the relation between resistance change and corrosion rate of a cylindrical specimen can be derived rather easily, starting with the relation between resistance and resistivity

$$R = \rho \frac{l}{A} = \frac{\rho l}{\pi r_o^2} \qquad (1)$$

where R is the resistance, l is the length and r_o is the original radius of the specimen. If the radius is reduced to r by uniform corrosion after an exposure period of t, then the change in resistance is

$$\Delta R = \frac{\rho l}{\pi r^2} - \frac{\rho l}{\pi r_o^2} \qquad (2)$$

Differentiating equation (2) with respect to time

$$\frac{d\Delta R}{dt} = -\frac{2\rho l}{\pi} \frac{1}{r^3} \frac{dr}{dt} \qquad (3)$$

$$-\frac{dr}{dt} = \frac{\pi r^3}{2\rho l} \frac{d\Delta R}{dt} \qquad (4)$$

from equation (2)

$$r = \left[\frac{\rho l r_o^2}{\pi r_o^2 \Delta R + \rho l} \right]^{1/2} \qquad (5)$$

substituting equation (5) into (4) gives

$$-\frac{dr}{dt} = \frac{\pi}{2\rho l} \left[\frac{1}{\frac{1}{r_o^2} + \frac{\pi}{\rho l} \Delta R} \right]^{3/2} \frac{d\Delta R}{dt}$$

Where corrosion is not uniform, it is necessary to take account of the non-uniformity by use of some type of correction factor.

References

(1) G. L. Booman, Analytical Chemistry 29, 213-218 (1957).

(2) J. M. Kolotyrkin, Journal of the Electrochemical Society 108, 209-216.

(3) H. Kaesche, Zeitschrift fur Physicalische Chemie 34, 87-108 (1962).

(4) J. F. Whiting and T. E. Wright, Corrosion 17, 8, (1961).

(5) R. H. Brown, Conference Paper Presented at the 30th Spring Meeting of the American Society of Refrigerating Engineers, Cleveland, Ohio, June 1, 1943.

(6) E. Deltombe and M. Pourbaix, Corrosion 14, 496 t, (1958).

(7) M. H. Peterson, J. A. Smith, B. F. Brown, "Effects of Electrochemical Potential on Stress-Corrosion Cracking of Aluminum Alloy 7079-T6 in Salt Water". Paper presented at the Second International Congress on Metallic Corrosion, New York, New York, March 1963.

(8) T. P. Hoar, Corrosion 19, 331 t (1963).

TABLE I

CHEMICAL ANALYSIS AND PROPERTIES OF TWO-INCH THICK 7075-T6 AND -T73 ALLOY PLATE

Chemical Analysis of Plate

Cu	Fe	Si	Mg	Mn	Zn	Ni	Cr	Ti	Be
1.62	0.20	0.09	2.63	0.04	5.92	0.00	0.17	0.02	0.001

Tensile Properties in Short-Transverse Direction and Electrical Conductivities

Temper	T.S. psi	Y.S. psi	El. % in 0.5"	Conductivity % IACS
-T6	82,400	74,600	2.0	31.0
-T73	71,500	65,800	2.9	38.5

Note: Blanks (1/4" x 1/4" x 2") taken in the short-transverse direction from two-inch thick 7075-T651 alloy plate were reheat treated one hour at 870°F, quenched in cold water and then artificially aged to the -T6 and -T73 tempers.

TABLE II

EFFECT OF DISSOLVED CORROSION PRODUCT ON THE CORROSION AND STRESS CORROSION OF 7075-T6

Solution (a)	Potential, Volts S.C.E.	Stress Level, % Yield Strength	Time to Failure, Hours	Corrosion Rate microhms/hr.
Fresh	Free corrosion (-0.75)	Unstressed	--	2.4
Fresh + 5 ppm Cu	Free corrosion (-0.75)	Unstressed	--	2.6
Fresh	Free corrosion (-0.75)	75	1.4, 1.0	
Old (5 ppm Cu)(b)(c)	Free corrosion (-0.75)	75	0.5	
Fresh	-1.15	75	5.0, 4.3	
Fresh + 5 ppm Cu (c)	-1.15	75	2.9	
Fresh + 25 ppm Cu (c)	-1.15	75	3.2, 1.3	

Notes: (a) The electrolyte contained 1 mole/liter NaCl, 0.2 mole/liter $AlCl_3$, with the pH adjusted to 1 with HCl.
(b) Estimated by qualitative spectrographic analysis and polarization tests.
(c) The copper content was obtained by dissolving the appropriate amount of 7075.

Figure 1

Diagram of apparatus for cathodic protection experiments.

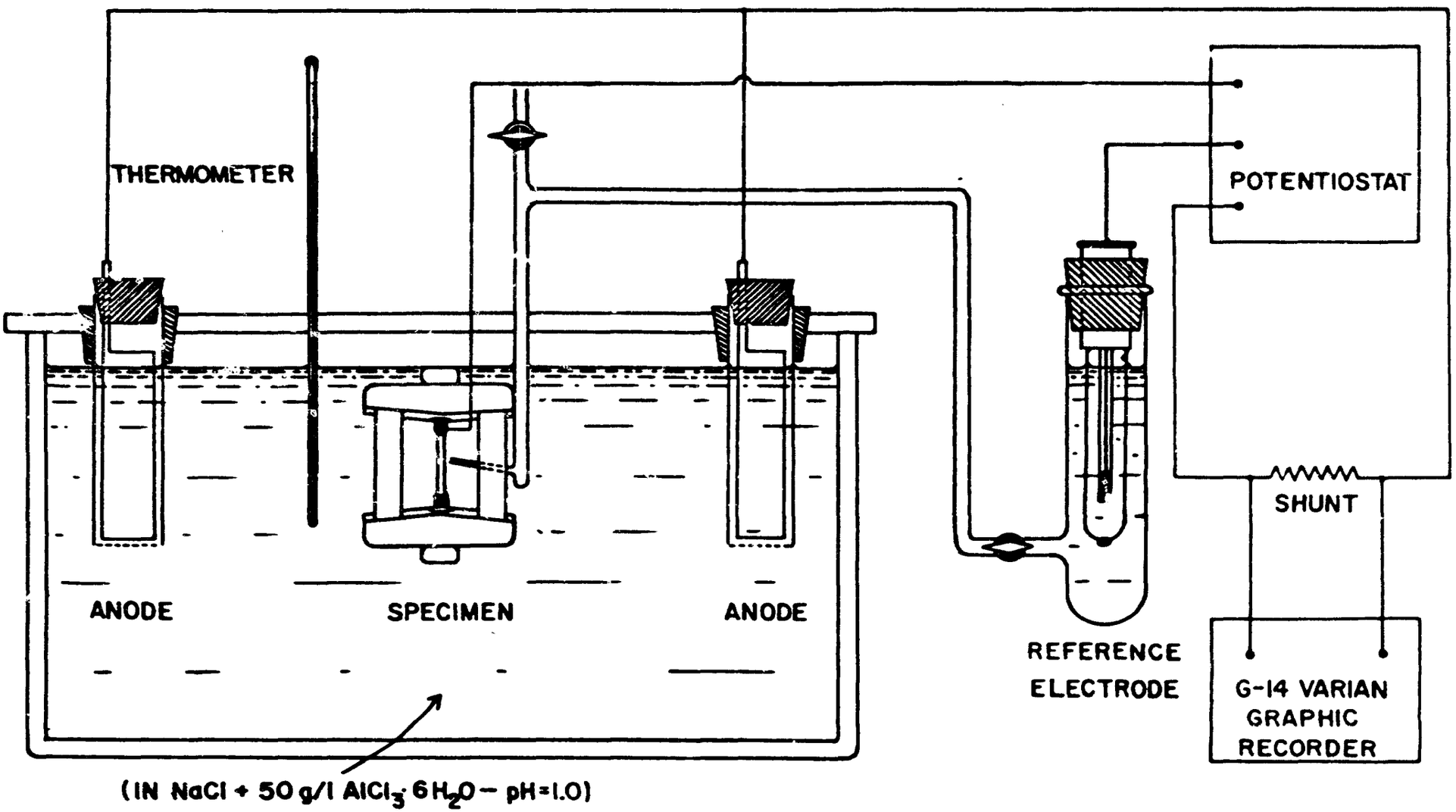
THERMOMETER
POTENTIOSTAT
SHUNT
ANODE
SPECIMEN
ANODE
REFERENCE
ELECTRODE
G-14 VARIAN
GRAPHIC
RECORDER
(IN NaCl + 50 g/l AlCl3·6H2O – pH=1.0)

Fig. 1

Figure 2

Diagram of circuit for measuring the electrical resistance and the time to failure of a specimen.

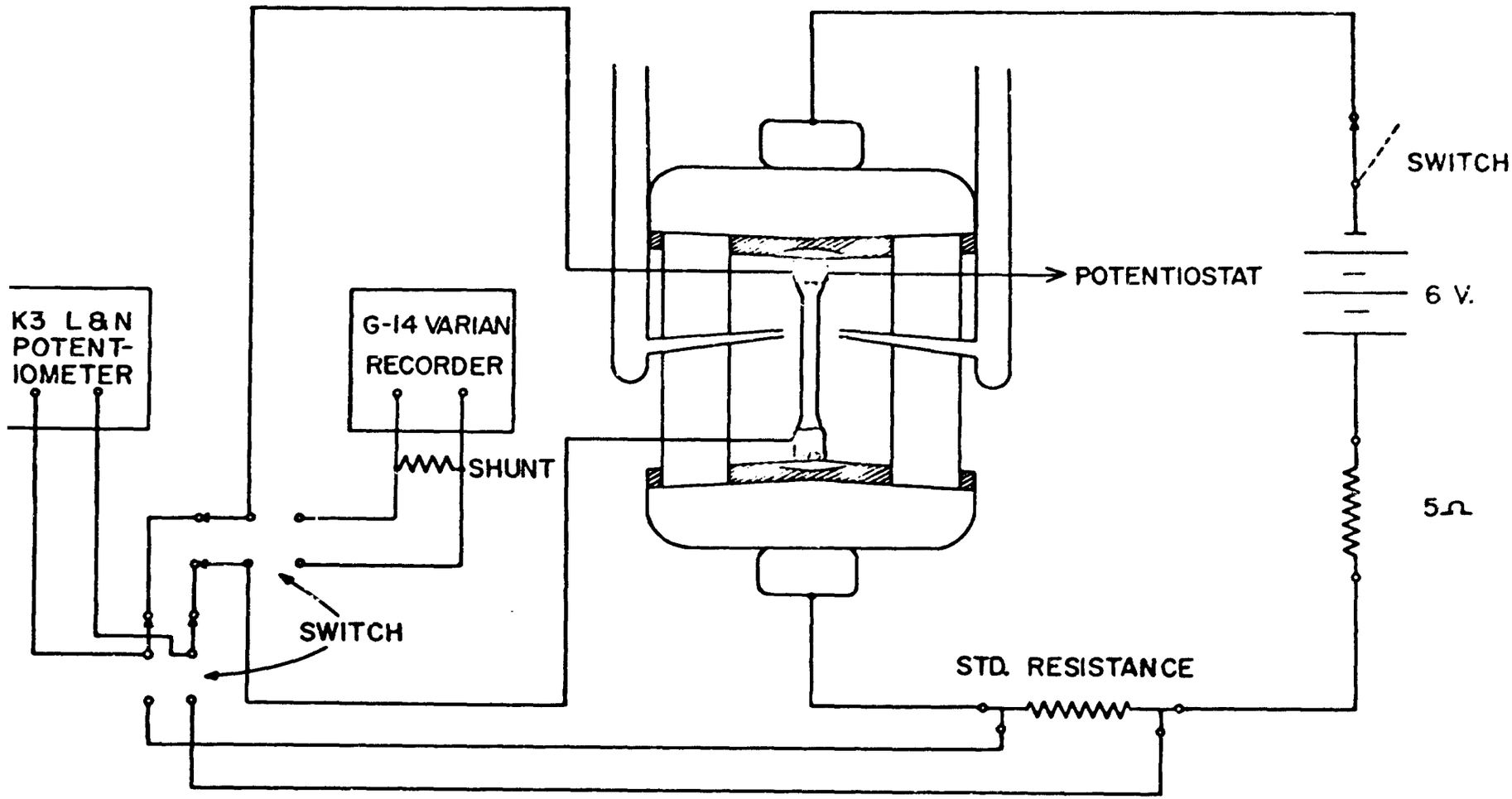
K3 L&N
POTENT-
IOMETER
G-14 VARIAN
RECORDER
SHUNT
SWITCH
POTENTIOSTAT
SWITCH
6 V.
5Ω
STD. RESISTANCE

Fig. 2

Figure 3

Photographs of stressed specimens showing percussion welded connectors (A), Luggin capillaries (B) and wax coating (C).

Figure 4

A typical resistance vs. time plot illustrating the spread of experimental readings.

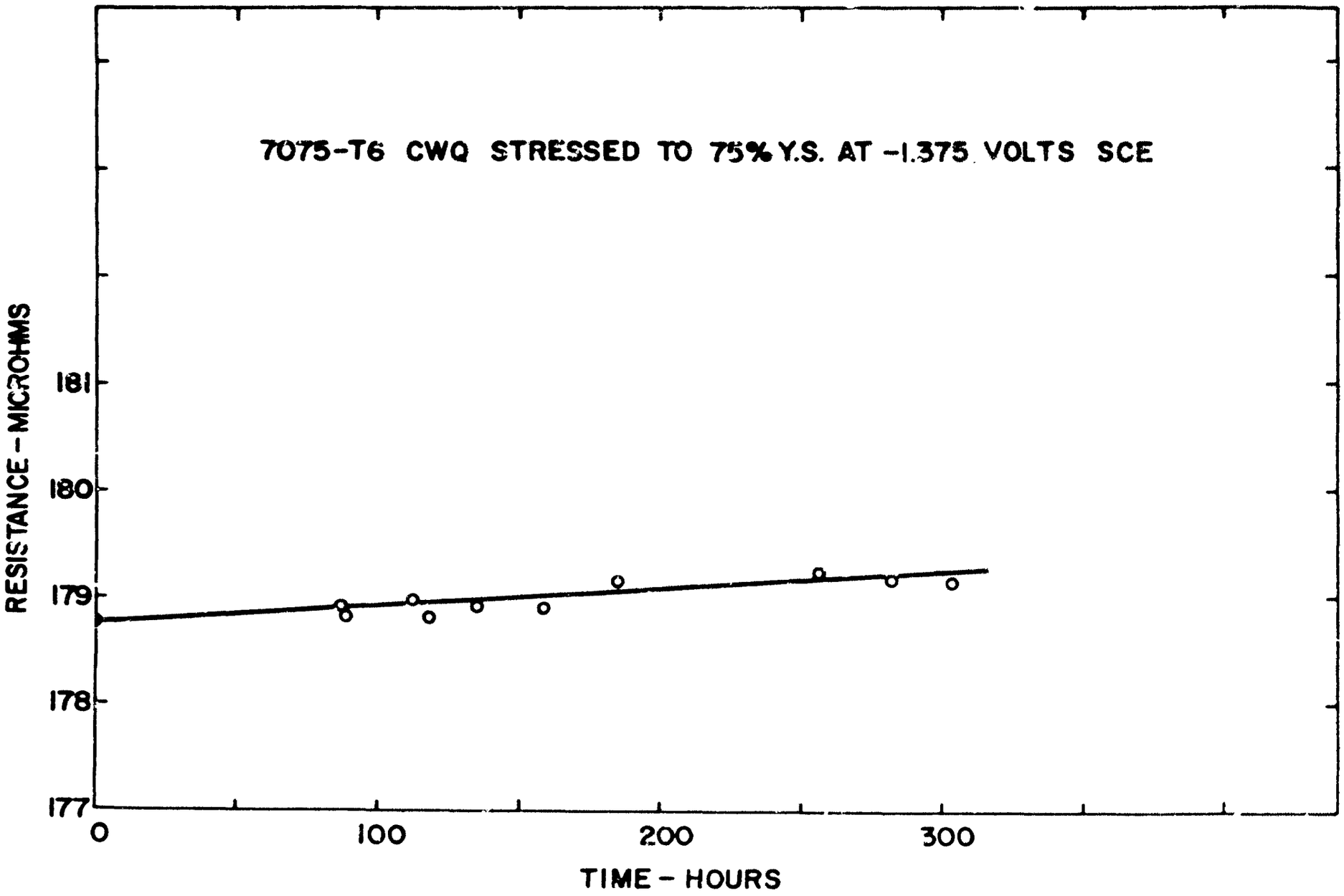
7075-T6 CWQ STRESSED TO 75% Y.S. AT -1.375 VOLTS SCE
RESISTANCE - MICROHMS
181
180
179
178
177
0
100
200
300
TIME - HOURS

Fig. 4

Figure 5

Effect of applied cathodic potential on the stress-corrosion performance of stressed short-transverse specimens from 7075-T6 alloy plate.

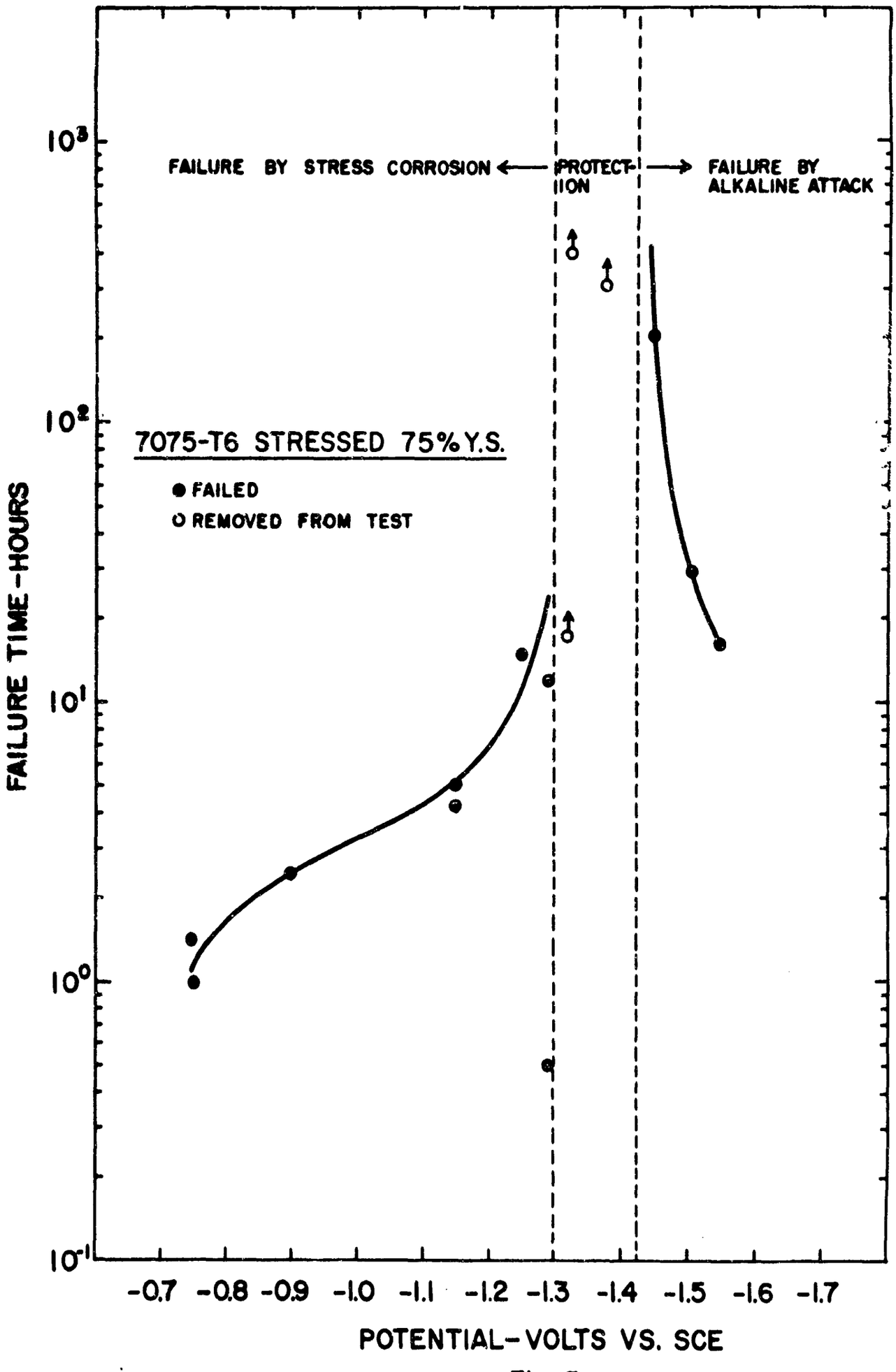
FAILURE BY STRESS CORROSION
PROTECTION
FAILURE BY ALKALINE ATTACK
7075-T6 STRESSED 75% Y.S.
● FAILED
○ REMOVED FROM TEST
FAILURE TIME-HOURS
10^3
10^2
10^1
10^0
10^{-1}
-0.7 -0.8 -0.9 -1.0 -1.1 -1.2 -1.3 -1.4 -1.5 -1.6 -1.7
POTENTIAL-VOLTS VS. SCE

Fig. 5

Figure 6

Effect of applied cathodic potential on the corrosion rate of short-transverse specimens from 7075-T6 and -T73 alloy plate. The points include both unstressed and stressed specimens.

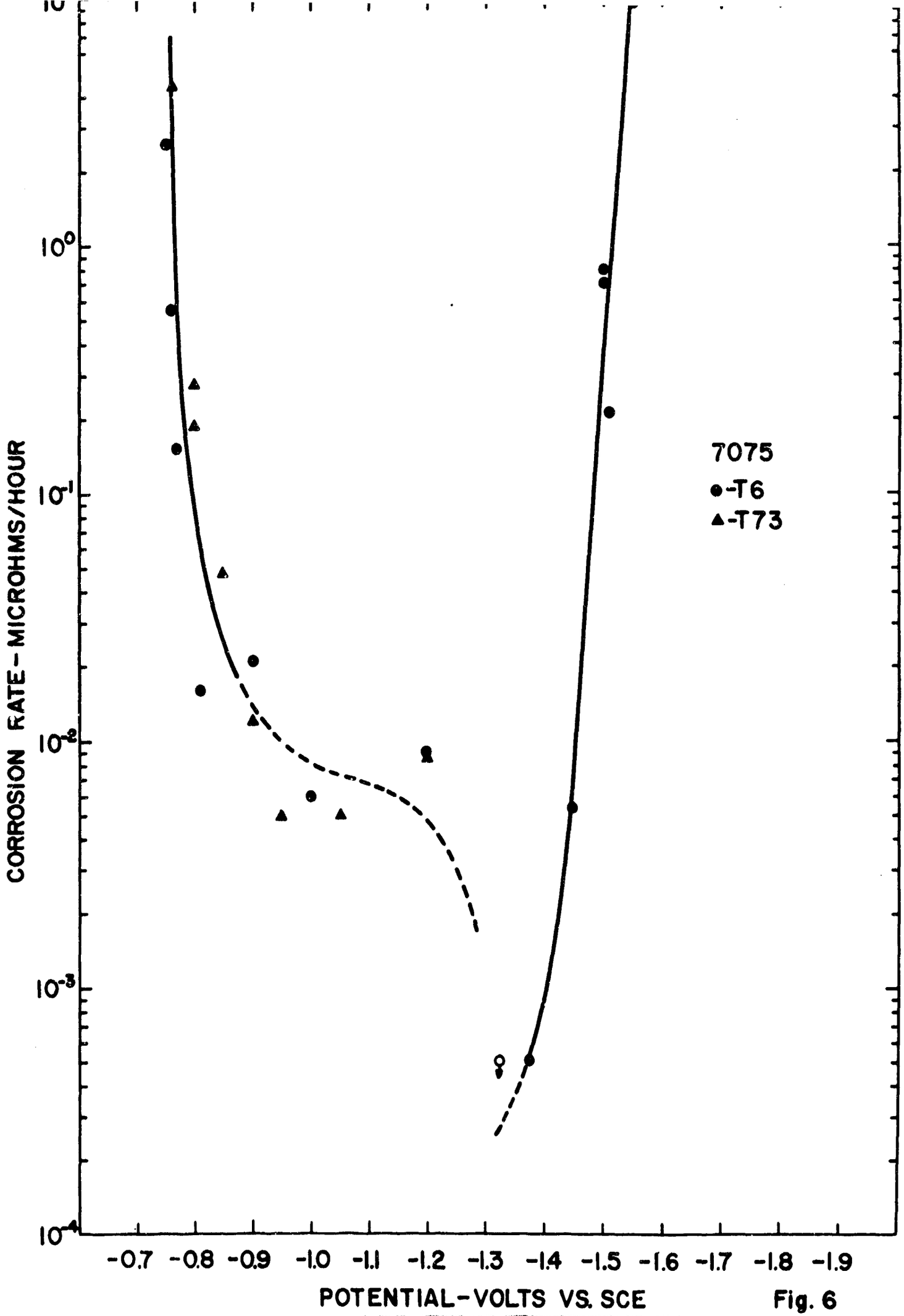
CORROSION RATE-MICROHMS/HOUR
10^{0}
10^{-1}
10^{-2}
10^{-3}
10^{-4}
7075
●-T6
▲-T73
-0.7 -0.8 -0.9 -1.0 -1.1 -1.2 -1.3 -1.4 -1.5 -1.6 -1.7 -1.8 -1.9
POTENTIAL-VOLTS VS. SCE

Fig. 6

Figure 7

Micrographs of sections through freely corroding 7075-T6 and -T73 specimens.

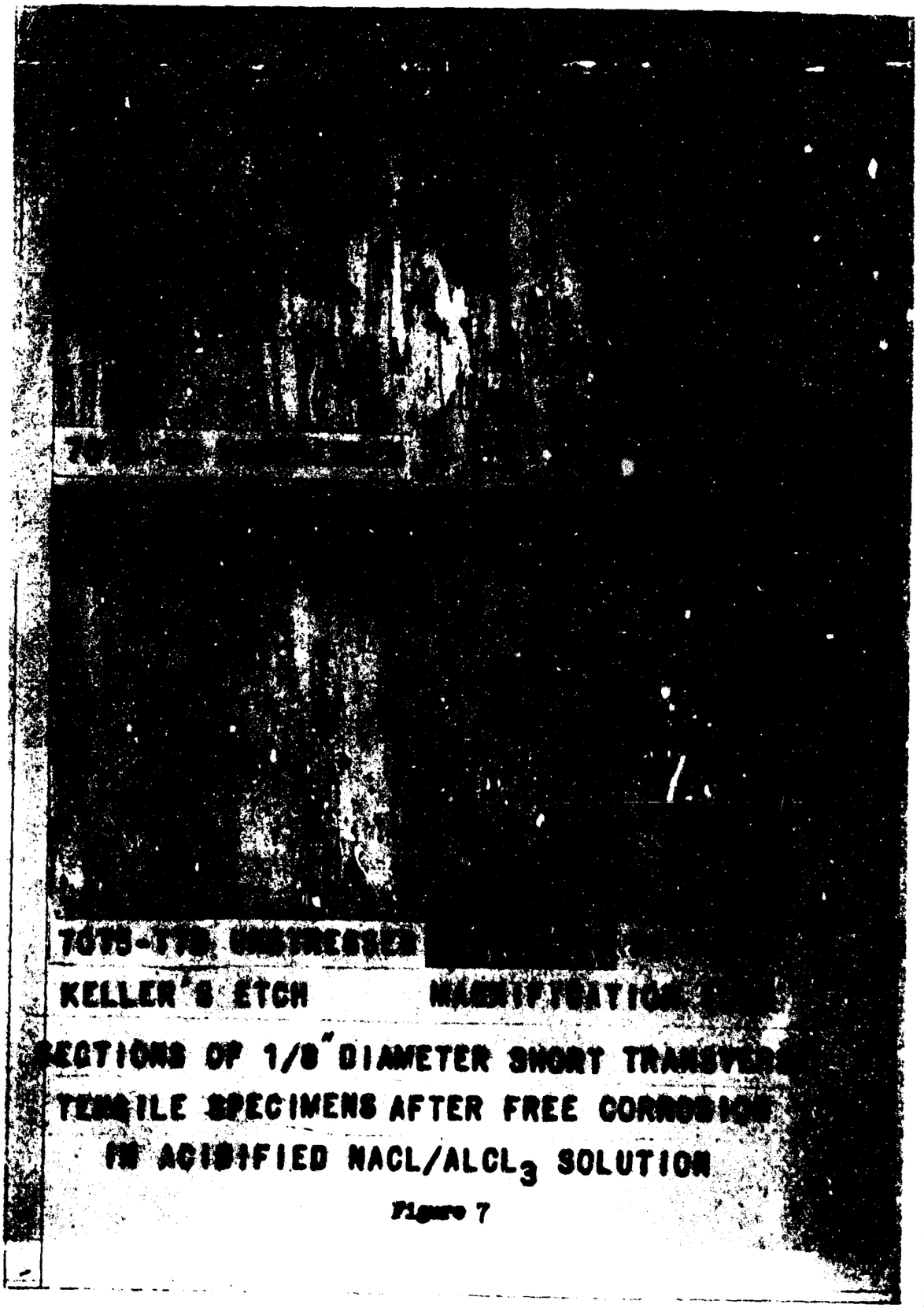

KELLER'S ETCH

SECTIONS OF 1/8" DIAMETER SHORT TRANSVERSE

TENSILE SPECIMENS AFTER FREE CORROSION

IN ACIDIFIED NACL/$ALCL_3$ SOLUTION

Figure 7

Figure 8

Resistance vs. time plots for freely corroding specimens illustrating the effect of stress.

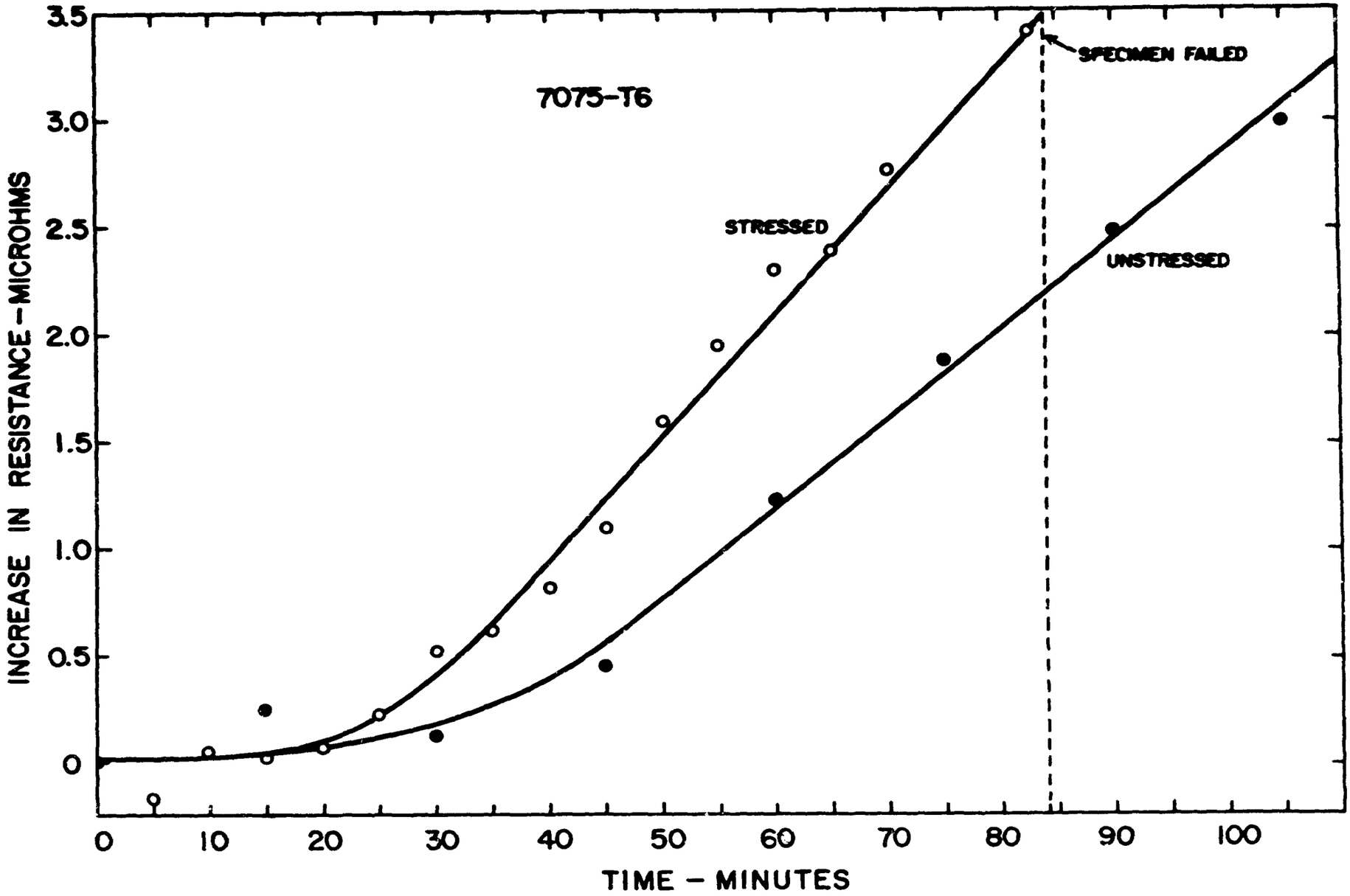
7075-T6
SPECIMEN FAILED
STRESSED
UNSTRESSED
INCREASE IN RESISTANCE - MICROHMS
TIME - MINUTES
0
0.5
1.0
1.5
2.0
2.5
3.0
3.5
0
10
20
30
40
50
60
70
80
90
100

Fig. 8

Figure 9

Effect of dissolved corrosion product on the current associated with cathodically protected specimens.

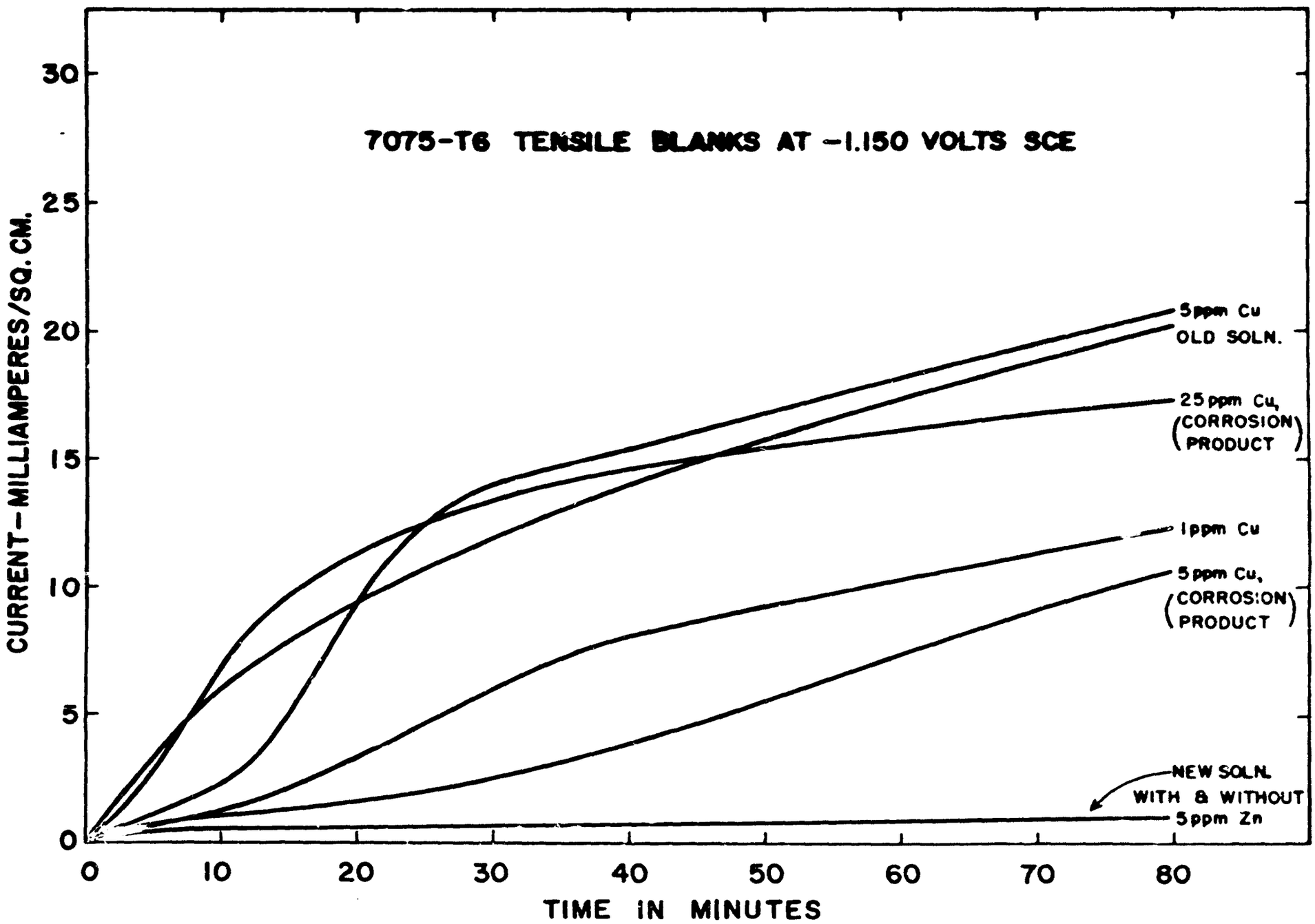
7075-T6 TENSILE BLANKS AT -1.150 VOLTS SCE
CURRENT-MILLIAMPERES/SQ.CM.
TIME IN MINUTES
0
5
10
15
20
25
30
0
10
20
30
40
50
60
70
80
5ppm Cu
OLD SOLN.
25ppm Cu,
(CORROSION
PRODUCT)
1ppm Cu
5ppm Cu,
(CORROSION
PRODUCT)
NEW SOLN.
WITH & WITHOUT
5ppm Zn

Fig. 9

Figure 10

Micrographs of sections through stressed 7075-T6 specimens cathodically protected at various potentials. Note the stress-corrosion crack in "A" indicated by an arrow and the small pits in "B" also indicated by arrows. Pitting could not be detected in "C" or "D". The pitting in "E" resulted from overprotection.

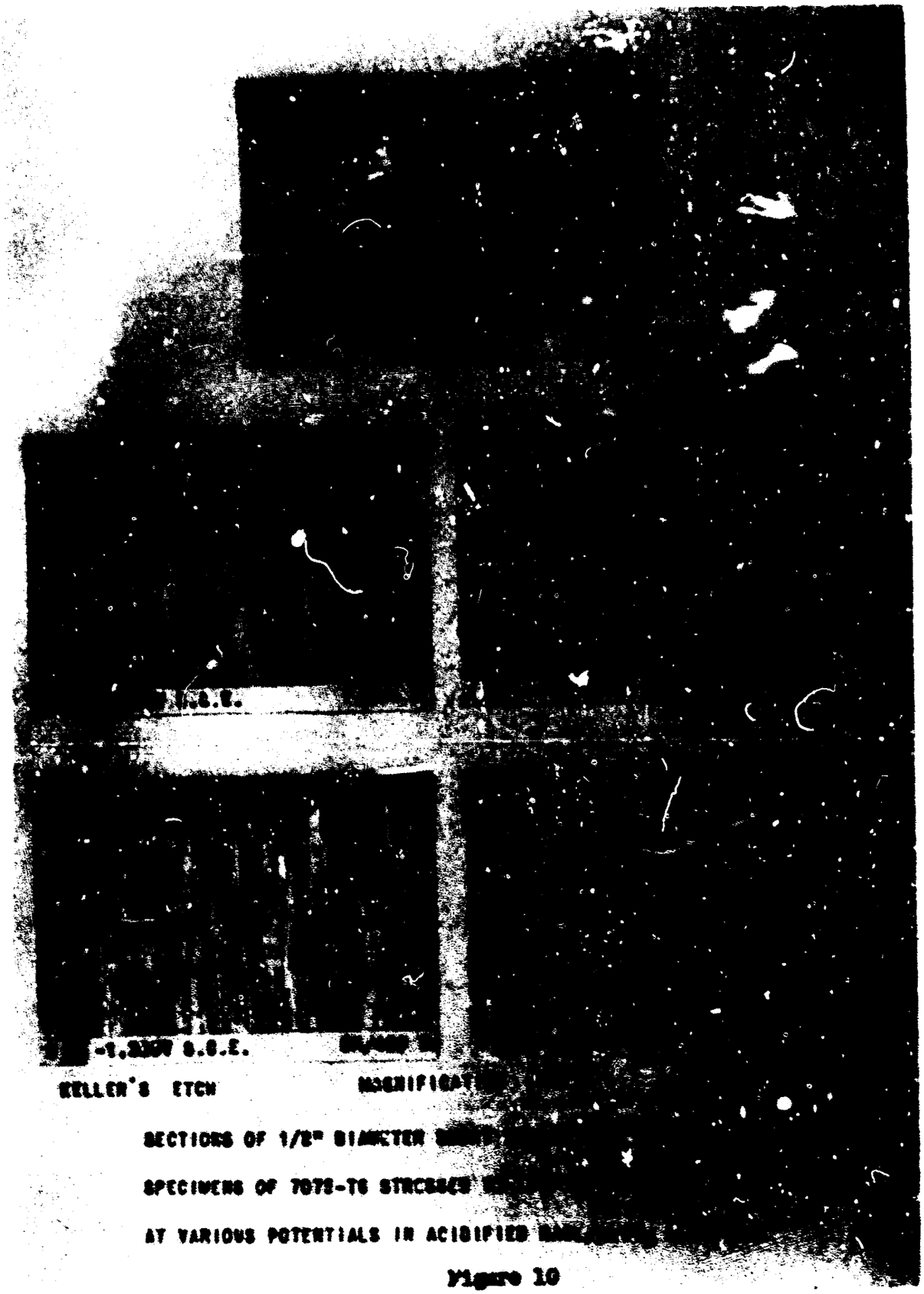

KELLER'S ETCH

SECTIONS OF 1/8" DIAMETER

SPECIMENS OF 7079-T6 STRESSED

AT VARIOUS POTENTIALS IN ACIDIFIED

Figure 10

Distribution List for Contract NOw64-0170c

1. Bureau of Naval Weapons
   Department of the Navy
   Washington 25, D. C.
   Internal distribution to be made by DLI-3 as follows:
   RRMA-222 (3 copies plus remainder after distribution)
   RRMA-5

2. Defense Documentation Center for Scientific & Technical Information (DDC)
   Arlington Hall Station
   Arlington 12, Virginia
   Attn: Document Service Center (TICSP) - (12 copies) (with a note stating "No Restrictions for DDC Distribution)

3. Bureau of Ships
   Department of the Navy
   Washington 25, D. C.
   Attn: Code 342B

4. Office of Naval Research
   Department of the Navy
   Washington 25, D. C.
   Attn: Code 423

5. Naval Air Material Center
   Aeronautical Materials Laboratory
   Philadelphia 12, Pennsylvania

6. Air Force Materials Laboratory
   Research & Technology Division
   Wright Patterson Air Force Base
   Ohio 45433
   Attn: MAMD
   MAAE

7. National Aeronautics & Space Administration
   Federal Building #10
   Washington, D. C. 20546
   Attn: Code RRM

8. Technical Information Service Extension
   U. S. Atomic Energy Commission
   P. O. Box 62
   Oak Ridge, Tennessee

9. Director
   National Bureau of Standards
   Washington 25, D. C.

10. Commanding Officer
    Office of Ordnance Research
    Box CM, Duke Station
    Durham, North Carolina

11. Army Materials Research Agency
Watertown Arsenal
Watertown, Massachusetts

12. U. S. Atomic Energy Commission
Document Library
Germantown, Maryland

13. Battelle Memorial Institute
505 King Avenue
Columbus 1, Ohio

14. U. S. Naval Research Laboratory
Washington 25, D. C.

15. U. S. Naval Ordnance Laboratory
White Oak, Silver Spring, Maryland
Attn: WM Division

16. Dow Metal Products Company
Midland, Michigan

17. Missile & Space Flight Center
P. & V. E. Labs.
Huntsville, Alabama
Attn: Mr. J. G. Williamson

18. Kaiser Aluminum & Chemical Corp.
Dept. of Metallurgical Research
Spokane, Washington 99215
Attn: Mr. T. R. Pritchett

19. Reynolds Metals Company
6601 West Broad Street
Reynolds Building
Richmond 18, Virginia
Attn: Mr. Harry Jackson (MRL)

20. IIT Research Institute
Metals Research Dept.
10 West 35th Street
Chicago, Illinois 60616
Attn: Dr. F. A. Crossley

21. Mr. Abner R. Willmer
Chief of Metals Research
David Taylor Model Basin
Washington 7, D. C.

22. Commanding Officer
Frankford Arsenal
Philadelphia, Pennsylvania
Attn: Mr. H. Markus
1320 Bldg. 64-4.